JOURNAL OF Materials CHEMISTRY

The *in-situ* synthesis process and luminescence behavior of a *p*-hydroxybenzoic acid–terbium complex in sol–gel derived host materials

Xianping Fan,[a,b] Xuhui Lv,[a] Shaobin Li,[a] Feng Wang[a] and Minquan Wang[a,b]

[a]*Department of Materials Science and Engineering, Zhejiang University, Hangzhou, 310027, P. R. China*
[b]*State Key Laboratory of Silicon Materials, Zhejiang University, Hangzhou, 310027, P. R. China*

Received 27th May 2002, Accepted 29th August 2002
First published as an Advance Article on the web 27th September 2002

The *in-situ* synthesis and photophysical properties of a *p*-hydroxybenzoic acid–terbium (PHBA–Tb^{3+}) complex in sol–gel derived host materials have been investigated. The Raman scattering spectrum of a 1% $TbCl_3$–3% PHBA co-doped gel was the same as that of the PHBA–Tb^{3+} complex powders synthesized in ethanolic solution, indicating that the PHBA–Tb^{3+} complex was synthesized in the 1% $TbCl_3$–3% PHBA co-doped gel. The steady-state excitation and emission spectra of the 1% $TbCl_3$–3% PHBA co-doped gel, which were similar to those of the PHBA–Tb^{3+} complex powders, also indicated the synthesis of the PHBA–Tb^{3+} complex in the 1% $TbCl_3$–3% PHBA co-doped gel. The time-resolved spectra of the 1%$TbCl_3$–3% PHBA co-doped gel indicated an efficient ligand-to-metal energy transfer, which also confirmed the synthesis of the PHBA–Tb^{3+} complex in the gel. The luminescence decay curve of the 1% $TbCl_3$–3% PHBA co-doped gel could be fitted by a double-exponential function. Due to the less efficient non-radiative $^5D_4$ relaxation processes in the gel, the presence of the PHBA–Tb^{3+} complex in the gel led to greatly increased $^5D_4$ lifetimes.

1. Introduction

The interest in the photophysical properties of lanthanide complexes with organic ligands has been greatly intensified after Lehn's proposition that such complexes could be seen as light-conversion molecular devices (LCMDs).[1] The emission of these lanthanide complexes usually results from the absorption of energy in the broad absorption band of the organic ligand followed by efficient transfer of this energy to an excited state of the central lanthanide ion, thus overcoming the very small absorption coefficients of the lanthanide ions. The transfer is then followed by emission from one or more of these excited states. Efficient LCMDs may find many applications, such as luminescent labels in fluoroimmunoassays, antireflection coatings on solar cells, lasers, or cheaper phosphors for fluorescent lighting.[2,3] In general, however, lanthanide complex solids are soft and soluble, and lack the mechanical properties desired to be used directly as luminescent sources. These problems are expected to be solved by doping the lanthanide complexes into suitable solid matrices.

The sol–gel method has been recently employed for the preparation of lanthanide-complex-dispersed composite materials.[4–12] These lanthanide-complex-dispersed composite materials have been observed to exhibit substantially improved luminescence characteristics with respect to comparable materials containing simple metal salts. The thermal stability of the complexes is improved, and the mechanical properties of the composite materials are also strengthened after the incorporation. Two approaches have been used to prepare lanthanide-complex-doped sol–gel materials. One approach is the synthesis of lanthanide complexes under general synthetic conditions and then to dissolve the synthesized lanthanide complexes in a solvent that is compatible with silicon alkoxide sol–gel preparative techniques.[4] The other approach is the *in-situ* synthesis of the lanthanide complexes during the sol–gel process.[5,6,9,12] In previous work, we have investigated the synthesis process of some lanthanide complexes in the gel and the luminescence behavior of the resulting composite materials.[5,6,9,12] Until now, however, there have been no direct spectroscopic data to confirm that the metal ion has been coordinated with the organic ligands during the *in-situ* synthesis of the lanthanide complexes. In this work, Raman scattering spectra are used to provide direct evidence that a *p*-hydroxybenzoic acid–terbium (PHBA–Tb^{3+}) complex has been *in-situ* synthesized in the sol–gel derived host materials and the photophysical properties of the PHBA–Tb^{3+} complex doped gel are described.

2. Experimental

2.1. Chemical synthesis of the PHBA–Tb^{3+} complex in ethanolic solution

Pure *p*-hydroxybenzoic acid–terbium complex powders were conventionally prepared by the addition of an ethanolic solution of *p*-hydroxybenzoic acid, $C_7H_6O_3$ (PHBA), to an ethanol solution containing $TbCl_3{\cdot}nH_2O$; $C_7H_6O_3$: $TbCl_3{\cdot}nH_2O$ = 3 : 1. The pH was adjusted to 6–7 with dilute NaOH aqueous solution. After refluxing for several hours the precipitate was filtered, washed, recrystallized in ethanol and dried at 40 °C. The process yields solid state PHBA–Tb^{3+} complex powders suitable for measurements.

2.2. Sol–gel preparations

Tetraethoxysilane, $Si(OC_2H_5)_4$ (TEOS), ethanol (C_2H_5OH) and distilled deionized water (H_2O) were used as starting materials to prepare the PHBA–Tb^{3+} complex doped gel. TEOS, C_2H_5OH and H_2O were mixed at the ratio of TEOS : C_2H_5OH : H_2O = 1 : 4 : 4. A small amount of HCl was added to the solution to promote hydrolysis. The PHBA was dissolved in ethanol in advance and was added to the solution with ethanol, the $TbCl_3{\cdot}nH_2O$ was then also introduced into the solution. The mixed solution was vigorously stirred for 1 h

 DOI: 10.1039/b205055b

at room temperature. The resulting sol was subsequently kept in a sealed container at 40 °C until the onset of gellation. Aging and drying were allowed to proceed under ambient conditions over a period of several weeks.

2.3. Instrumentation

The steady-state excitation and emission spectra were measured using a Hitachi F-3010 fluorescence spectrophotometer. The luminescence decay curves were carried out with PTI TimeMaster™ fluorescence lifetime spectrometers. Infrared spectra were obtained using an FTIR Nicolet Avatar 360 spectrometer. The Raman scattering spectra were measured with a PerkinElmer System 2000NIR FT-Raman spectrometer. To measure the time-resolved spectra, the samples were excited by the emission line at 355 nm from a YAG laser (Model Tempest 20 Hz, New Wave). The resulting fluorescence was analyzed by a 0.75 m grating monochromator/photomultiplier (Model SP-750, Action Research Corporation) and then read out by a boxcar (Model SR250, Stanford Research System, Inc.). The delay time was defined as the time between the onset of the excitation laser pulse and the trigger of the boxcar sampling and was controlled by a delay pulse generator (Model DG535, Stanford Research System, Inc.). All measurements were made at room temperature.

3. Results and discussion

The elemental analysis results indicated that the PHBA–Tb^{3+} complex powder synthesized in ethanolic solution was $Tb(C_7H_5O_3)_3{\cdot}2H_2O$. (Exp.: C = 41.46, H = 3.62. Calc.: C = 41.58, H = 3.14). Fig. 1 shows the infrared absorption spectra of the PHBA and the PHBA–Tb^{3+} complex powders that were synthesized in ethanolic solution. The main absorption band assignment is shown in Table 1.[13] The bands corresponding to the $\nu_{C=O}$ and the ν_{C-O} for the –COOH of the PHBA were situated at 1684 cm^{-1} and 1264 cm^{-1}, respectively. The two bands disappeared in the PHBA–Tb^{3+} complex. The band corresponding to the γ_{OH} in the –COOH of the PHBA was situated at 930 cm^{-1}. This band also disappeared in the PHBA–Tb^{3+} complex. The bands at 617, 770 and 852 cm^{-1} corresponding to the δ_{CH} of the PHBA moved towards higher wavenumbers, 630, 790 and 856 cm^{-1}, in the PHBA–Tb^{3+} complex. Carboxylic acid salts have a very

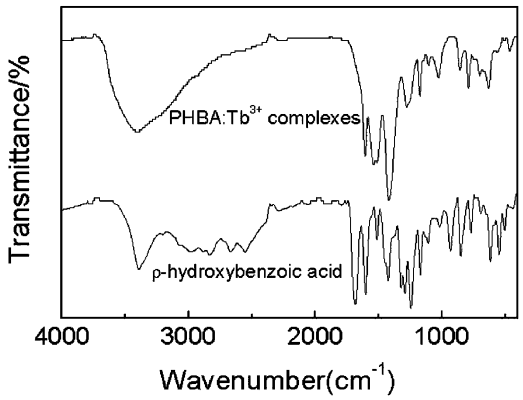

Fig. 1 Infrared absorption spectra of PHBA and PHBA–Tb^{3+} complex synthesized in ethanolic solution.

Table 1 Infrared wavenumbers and absorption band assignments

ν/cm^{-1}	Assignment	ν/cm^{-1}	Assignment
615–910	δ_{CH}	1400–1420	$\nu_{s(-COO-)}$
900–940	γ_{OH}	1550–1610	$\nu_{as(-COO-)}$
1200–1320	ν_{C-O}	1680–1760	$\nu_{C=O}$ of monomer and dimer

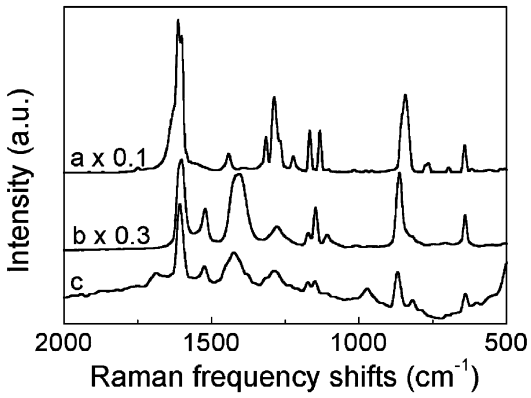

Fig. 2 Raman scattering spectra of: (a) PHBA; (b) PHBA–Tb^{3+} complex; and (c) 1% $TbCl_3$–3% PHBA co-doped gel.

strong, characteristic band in the 1610–1550 cm^{-1} region due to the asymmetric stretching vibration of $-CO_2^-$ The symmetric stretching vibration of this group gives rise to a band in the range 1420–1335 cm^{-1} and is of medium intensity, broad, and generally has two or three peaks.[14] Therefore, the strong absorption band at 1420 cm^{-1} corresponding to the $\nu_{s(-COO-)}$ of the PHBA–Tb^{3+} complex and the bands at 1606 cm^{-1} and 1550 cm^{-1} corresponding to the $\nu_{as(-COO-)}$ of the PHBA–Tb^{3+} complex also indicated the synthesis of the PHBA–Tb^{3+} complex. On the other hand, the broad band at 3000–3600 cm^{-1} corresponding to free OH stretching vibrations also indicated that the synthesized PHBA–Tb^{3+} complex contained water molecules.

Fig. 2 shows the Raman scattering spectra of the PHBA, the PHBA–Tb^{3+} complex powders and the 1% $TbCl_3$–3% PHBA co-doped gel. Similar to the IR absorption spectra, the band at 842 cm^{-1} corresponding to the δ_{CH} of the PHBA moved towards higher wavenumbers (862 cm^{-1}) in the Raman scattering spectra of the PHBA–Tb^{3+} complex. The PHBA exhibited Raman shift peaks at 1287 cm^{-1} and 1315 cm^{-1} due to the C–O stretching vibration of the –COOH. The C=O stretching vibration of the PHBA gave rise to a Raman shift peak at 1612 cm^{-1}. After the PHBA–Tb^{3+} complex had been synthesized, these Raman shift peaks disappeared. Conversely, Raman shift peaks at 1520 and 1601 cm^{-1}, corresponding to the asymmetric stretching vibration of $-CO_2^-$, and at 1404 cm^{-1}, corresponding to the symmetric stretching vibration of $-CO_2^-$, can be observed in the Raman scattering spectra of the PHBA–Tb^{3+} complex. The Raman scattering spectra of the 1% $TbCl_3$–3% PHBA co-doped gel could be observed to be the same as that of the PHBA–Tb^{3+} complex. The Raman shift peaks at 1520 and 1601 cm^{-1}, corresponding to the asymmetric stretching vibration of $-CO_2^-$, and at 1404 cm^{-1}, corresponding to symmetric stretching vibration of $-CO_2^-$, can also be observed in the Raman scattering spectra of the 1% $TbCl_3$–3% PHBA co-doped gel, which indicates that the PHBA–Tb^{3+} complex has been synthesized in the 1% $TbCl_3$–3% PHBA co-doped gel.

Fig. 3 shows the steady-state excitation (monitored at 546 nm) and emission spectra of the PHBA–Tb^{3+} complex (excited at 312 nm), the 1% $TbCl_3$–3% PHBA co-doped gel (excited at 284 nm), and the 1% $TbCl_3$ doped gel (excited at 371 nm). The emission spectra of the PHBA–Tb^{3+} complex and the 1% $TbCl_3$–3% PHBA co-doped gel, which were the same as that of the $TbCl_3$ doped gel with respect to the positions, numbers and relative intensities of emission bands, consisted of a few narrow emission bands of Tb^{3+} ions. The emission bands of the Tb^{3+} ions have been assigned to transitions from the $^5D_4$ level to the $^7F_6$, $^7F_5$, $^7F_4$ and $^7F_3$ levels at 485, 546, 586 and 623 nm. However, the maximum intensity of the $^5D_4 \rightarrow {}^7F_5$ peak at 546 nm in the 1% $TbCl_3$–3% PHBA co-doped gel was observed

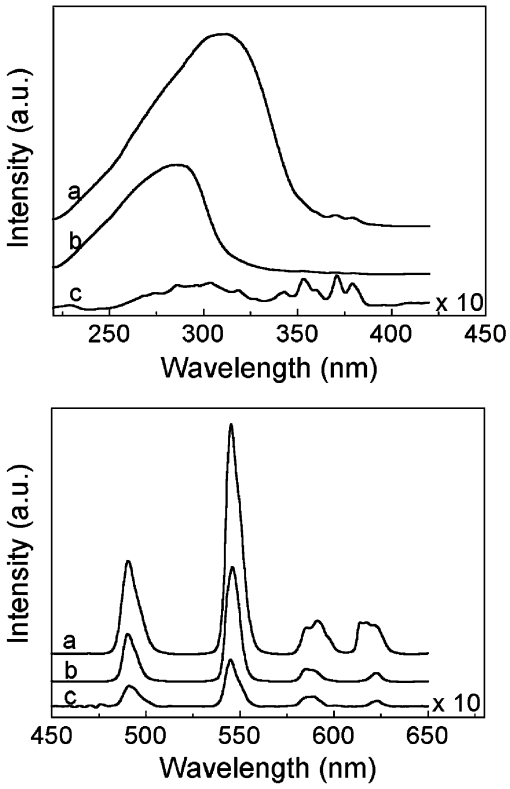

Fig. 3 Excitation (top) and emission (bottom) spectra of: (a) the PHBA–Tb^{3+} complex; (b) the 1% $TbCl_3$–3% PHBA co-doped gel; (c) the 1% $TbCl_3$ doped gel.

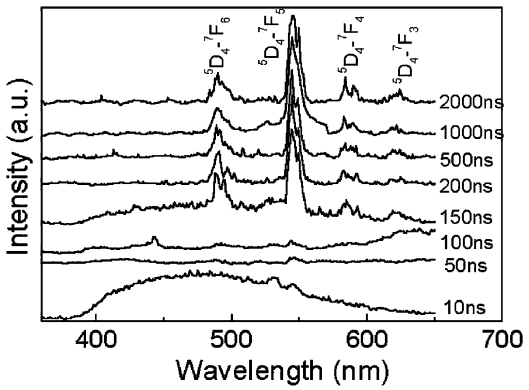

Fig. 4 Time-resolved spectra of the PHBA–Tb^{3+} complex.

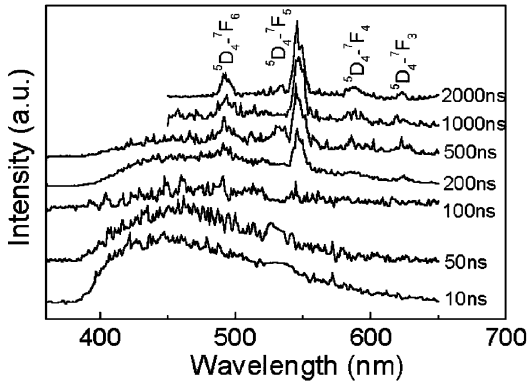

Fig. 5 Time-resolved spectra of the 1% $TbCl_3$–3% PHBA co-doped gel.

to be approximately 20 times more than that of the $TbCl_3$ doped gel.

The narrow excitation bands between 330 nm and 390 nm in the $TbCl_3$ doped gel resulted from the 4f–4f direct excitation band of Tb^{3+} ions. The broad excitation band of the PHBA–Tb^{3+} complex and the 1% $TbCl_3$–3% PHBA co-doped gel could be assigned to the excitation of the organic ligand PHBA from its ground electronic state to the lowest excited singlet state. Therefore, the excitation and emission spectra of the PHBA–Tb^{3+} complex and the 1% $TbCl_3$–3% PHBA co-doped gel indicated an efficient ligand-to-metal energy transfer, since the most intense feature in the excitation spectrum of the lanthanide complex is a broad band corresponding to transitions populating the ligand-centered excited states.[15] In addition, the 1% $TbCl_3$–3% PHBA co-doped gel can be found to have notably higher luminescence intensities than the 1% $TbCl_3$ doped gel, which indicated also an efficient ligand-to-metal energy transfer. It also indicated that the PHBA–Tb^{3+} complex has been synthesized in the 1% $TbCl_3$–3% PHBA co-doped gel.

Fig. 4 shows the emission spectra of the PHBA–Tb^{3+} complex at various delay times measured at room temperature. The spectra collected at short delay times exhibited only a broad band emission, which can be attributed to the radiative transitions of organic ligand PHBA. The sharp emission bands of the $^5D_4 \rightarrow {}^7F_J$, ($J$ = 6, 5, 4, 3) transitions of terbium ions could be observed at 150 ns delay, *i.e.* the characteristic time for the energy transfer from the PHBA to the terbium ions was about 150 ns. This means that the energy transfer from the PHBA to the terbium ions proceeds through a triplet ligand excited state because the ligand singlet to lanthanide ions energy transfer time is very fast when the ligand is directly coordinated to the metal centre. Fig. 5 shows the emission spectra of the 1% $TbCl_3$–3% PHBA co-doped gel at various delay times measured at room temperature. The spectra collected at short delay times also exhibited only a broad band emission and the broad band was still observed when the delay time was 200 ns. The broad band collected at longer delay times could be attributed to the delayed fluorescence of PHBA, which was induced by the radiative decay from the S_1 state to the S_0 state after thermal reactivation from the triplet state by reverse intersystem crossing. The broad band might also result from room temperature phosphorescence emission, which overlapped with the delayed fluorescence and was related to the radiative transition from the lowest triplet state T_1 to the S_0 state. Phosphorescence and delayed fluorescence for organic molecules in solution can often be observed only near liquid nitrogen temperatures. If organic molecules are entrapped in rigid surroundings to reduce the non-radiative pathways, however, room temperature phosphorescence and delayed fluorescence might be observed. Phosphorescence and delayed fluorescence at room temperature were recently observed for a number of organic dyes dispersed in sol–gel derived matrices.[16,17] Besides the room temperature phosphorescence and delayed fluorescence, some energy in the triplet state T_1 was also transferred to the excited state of the terbium ions which resulted in the emission of the terbium ions. The sharp emission bands of the $^5D_4 \rightarrow {}^7F_J$ (J = 6, 5, 4, 3) transitions of the terbium ions could be observed at 200 ns delay. Therefore, the time-resolved spectra of the 1% $TbCl_3$–3% PHBA co-doped gel also indicated the ligand-to-metal energy transfer, which also confirmed the synthesis of the PHBA–Tb^{3+} complex in the gel.

The luminescence decay curves of the $^5D_4$ state were obtained by monitoring the $^5D_4 \rightarrow {}^7F_5$ emission line for the PHBA–Tb^{3+} complex and for the 1% $TbCl_3$–3% PHBA co-doped gel. Fig. 6 shows the observed luminescence decay curves and the fitted curves for the PHBA–Tb^{3+} complex. The luminescence decay curve was best fitted to a double-exponential fitting function: $I(t) = 4543\exp(-t/96.8) + 741\exp(-t/242.4)$. Fig. 7 shows the observed luminescence decay curves and fitted

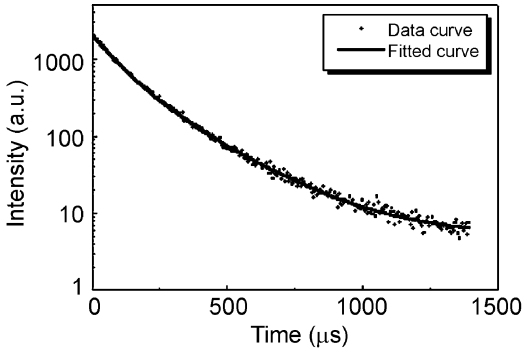

Fig. 6 Decay and fitted curves for the luminescence $^5D_4$ state of the PHBA–Tb^{3+} complex.

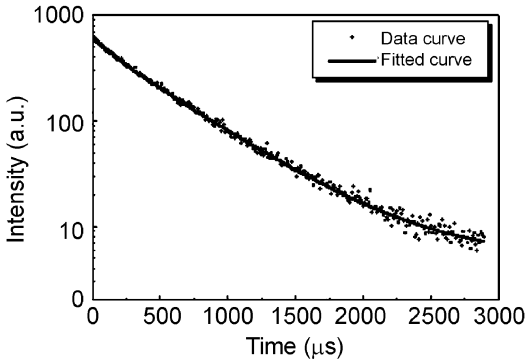

Fig. 7 Decay and fitted curves for the luminescence $^5D_4$ state of the 1% $TbCl_3$–3% PHBA co-doped gel.

curves for the 1% $TbCl_3$–3% PHBA co-doped gel. The luminescence decay curve was also best fitted by a double-exponential fitting function: $I(t) = 212.2\exp(-t/159.2) + 611.9\exp(-t/529.5)$. Obviously, the luminescence intensity $I(t)$ of the PHBA–Tb^{3+} complex and the 1% $TbCl_3$–3% PHBA co-doped gel could be described by the sum of two exponential decay components from:

$$I(t) = A_1 \exp\left(-\frac{t}{\tau_1}\right) + A_2 \exp\left(-\frac{t}{\tau_2}\right) \quad (1)$$

where τ_1 and τ_2 are the short- and long-decay components, respectively. Parameters A_1 and A_2 are fitting constants. According to eqn. (1), the average lifetime $\langle\tau\rangle$ is given by:

$$\langle\tau\rangle = \frac{A_1\tau_1^2 + A_2\tau_2^2}{A_1\tau_1 + A_2\tau_2} \quad (2)$$

where weight factors A_1 and A_2 are introduced. According to eqn. (2) the average lifetime of the PHBA–Tb^{3+} complex was 139 μs, and that of the 1% $TbCl_3$–3% PHBA co-doped gel was 480 μs. The results clearly show that the PHBA–Tb^{3+} complex in the gel led to greatly longer $^5D_4$ lifetimes. This can be ascribed to the less efficient non-radiative $^5D_4$ relaxation processes in the gel.

Transitions between f^n configuration states in lanthanide ions are parity forbidden transitions. The probabilities of such transitions are so low that the molar absorption coefficients are of the order of 1 and the radiative lifetimes are of the ms time scale. The experimental decay times are actually one or two orders lower than the estimated radiative lifetimes. This fact indicates that the decays of emitting states are mainly governed by non-radiative transitions. According to the theory of non-radiative transitions in lanthanide complexes,[18] the non-radiative relaxation between various J states may occur by interaction of the electronic levels of lanthanide ions with suitable vibrational modes of the environment. Therefore, the double exponential decay curves indicated that there are two different surroundings of the terbium ions. Elemental analysis showed that there were some water molecules coordinated to the terbium ion in the PHBA–Tb^{3+} complex. This coordination was also confirmed by the IR spectrum shown in Fig. 1. Besides being coordinated by organic ligands, therefore, the central terbium ions were also coordinated by water molecules in the PHBA–Tb^{3+} complex, leading to the double exponential decay curve.

A number of Si–OH groups are present in silica gels because the hydrolysis of alkoxides in the transition from sols to gels is incomplete.[19] Because these O–H groups may play the role of killers or trap centers in gels, various ligands are used with potential shielding properties. Such ligands should isolate the central lanthanide ion from O–H oscillators, which would lead to greatly enhanced quantum yields and longer decay times. The reactant $TbCl_3$ and PHBA were introduced to the sol successively. Thus the $TbCl_3$ and PHBA may be isolated in different pores of the silica network during the formation of the gels. Owing to the difficulty for the diffusion of the reactant $TbCl_3$ and PHBA between the pores, not all the reactant $TbCl_3$ and PHBA was used to synthesize the PHBA–Tb^{3+} complex in the 1% $TbCl_3$–3% PHBA co-doped gels. Thus, only some of the central terbium ions are isolated from O–H oscillators by the ligands. Therefore, there are two different surroundings for the central terbium ions in the 1% $TbCl_3$–3% PHBA co-doped gel; some are coordinated by O–H groups and others are coordinated by ligands, leading to the double exponential decay curve.

4. Conclusions

The Raman scattering spectrum has been used to confirm the synthesis of the PHBA–Tb^{3+} complex in the 1% $TbCl_3$–3% PHBA co-doped gel in comparison with the Raman scattering spectrum of the PHBA–Tb^{3+} complex powders synthesized in ethanolic solution. The steady-state excitation and emission spectra and the time-resolved spectra of the 1% $TbCl_3$–3% PHBA co-doped gel, which were similar to those of the PHBA–Tb^{3+} complex powders, indicated an efficient ligand-to-metal energy transfer, which also confirmed the synthesis of the PHBA–Tb^{3+} complex in the gel. The decay curve of the 1% $TbCl_3$–3% PHBA co-doped gel could be fitted by a double-exponential function. The PHBA–Tb^{3+} complex in the gel was observed to promote significantly longer $^5D_4$ lifetimes in comparison with PHBA–Tb^{3+} complex powders.

Acknowledgement

The authors gratefully acknowledge support for this research by the Chinese National Nature Science Foundation (No. 50072024)

References

1 J.-M. Lehn, *Angew. Chem., Int. Ed. Engl.*, 1990, **29**, 1304–1309.
2 C. de Mello Donegá, S. A. Junior and G. F. de Sá, *J. Chem. Soc., Chem. Commun.*, 1996, 1199–1200.
3 G. F. de Sá, S. A. Junior, B. J. P. da Silva and E. F. da Silva, Jr., *Opt. Mater.*, 1998, **11**, 23–28.
4 L. R. Matthews and G. H. Knobbe, *Chem. Mater.*, 1993, **5**, 1687–1691.
5 X. P. Fan, M. Q. Wang and Z. Y. Wang, *Mater. Res. Bull.*, 1997, **31**, 1119–1125.
6 G. D. Qian, M. Q. Wang, M. Wang, X. P. Fan and Z. L. Hong, *J. Mater. Sci. Lett.*, 1997, **16**, 322–324.
7 T. Jin, S. Tsutsumi, Y. Deguchi, K. Machida and G. Adachi, *J. Alloys Compd.*, 1997, **252**, 59–66.
8 J. M. Costa-Fernández, M. E. Diaz-García and A. Sanz-Medel, *Anal. Chim. Acta*, 1998, **360**, 17–26.

9 X. P. Fan, M. Q. Wang and Z. Y. Wang, *J. Phys. Chem. Solids*, 1999, **60**, 53–56.
10 T. Saraidarov, R. Reisfeld and M. Pietraszkiewicz, *Chem. Phys. Lett.*, 2000, **330**, 515–520.
11 R. Reisfeld, T. Saraidarov, M. Pietraszkiewicz and S. Lis, *Chem. Phys. Lett.*, 2001, **349**, 266–270.
12 X. P. Fan, Z. Y. Wang and M. Q. Wang, *Chem. Phys. Lett.*, 2002, **358**, 115–120.
13 Z. Wang, in *Modern Fourier Transform Infared Spectroscopy Technology and Application*, ed. J. Wu, Science and Technology Press, Beijing, 1994, p. 613.
14 G. Socrates, *Infrared Characteristic Group Frequencies*, Wiley, Chichester, 1980, p. 65.
15 G. F. de Sá, O. L. Malta, C. de Mello Donegá, A. M. Simas, R. L. Longo, P. A. Santa-Cruz and E. F. da Silva, Jr., *Coord. Chem. Rev.*, 2000, **196**, 165–195.
16 D. Levy and D. Avnir, *J. Photochem. Photobiol., A*, 1991, **57**, 41–45.
17 R. Reisfeld, M. Eyal and R. Gvishi, *Chem. Phys. Lett.*, 1987, **138**, 377–381.
18 N. Sabbatini and M. Guardigli, *Coord. Chem. Rev.*, 1993, **123**, 201–228.
19 A. M. Klonkowski, S. Lis, Z. Hnatejko, K. Czarnobaj, M. Pietraszkiewicz and M. Elbanowski, *J. Alloys Compd.*, 2000, **300–301**, 55–60.